

# MetaNODE: Prototype Optimization as a Neural ODE for Few-Shot Learning

Baoquan Zhang, Xutao Li, Yunming Ye, Shanshan Feng, Rui Ye

Harbin Institute of Technology, Shenzhen

zhangbaoquan@stu.hit.edu.cn

## Abstract

*Few-Shot Learning (FSL) is a challenging task, i.e., how to recognize novel classes with few examples? Pre-training based methods effectively tackle the problem by pre-training a feature extractor and then predict novel classes via a nearest neighbor classifier with mean-based prototypes. Nevertheless, due to the data scarcity, the mean-based prototypes are usually biased. In this paper, we diminish the bias by regarding it as a prototype optimization problem. Although the existing meta-optimizers can also be applied for the optimization, they all overlook a crucial gradient bias issue, i.e., the mean-based gradient estimation is also biased on scarce data. Consequently, we regard the gradient itself as meta-knowledge and then propose a novel prototype optimization-based meta-learning framework, called MetaNODE. Specifically, we first regard the mean-based prototypes as initial prototypes, and then model the process of prototype optimization as continuous-time dynamics specified by a Neural Ordinary Differential Equation (Neural ODE). A gradient flow inference network is carefully designed to learn to estimate the continuous gradients for prototype dynamics. Finally, the optimal prototypes can be obtained by solving the Neural ODE using the Runge-Kutta method. Extensive experiments demonstrate that our proposed method obtains superior performance over the previous state-of-the-art methods. Our code will be publicly available upon acceptance.*

## 1. Introduction

With abundant annotated data, deep learning techniques have shown very promising performance for many applications, e.g., image classification [17]. However, preparing enough annotated samples is very time-consuming, laborious, or even impractical in some scenarios, e.g., cold-start recommendation [47] and medical diagnose [28]. Few-shot learning (FSL), which aims to address the issue by mimicking the flexible adaptation ability of human to novel tasks from very few examples, has been proposed and received considerable attentions. Its main rationale is to learn meta-

knowledge from base classes with sufficient labeled samples and then employ the meta-knowledge to perform class prediction for novel classes with scarce examples [21].

Previous studies primarily address the FSL problem using the idea of meta-learning, i.e., constructing a large set of few-shot tasks on base classes to learn task agnostic meta-knowledge [15, 22, 42]. Recently, Chen et al. regard feature representation as meta-knowledge, and propose a simple pre-training method [9], which delivers more promising performance. In the method, they first pre-train a feature extractor on all base classes, and then perform novel class prediction via mean-based prototypes in the feature space. However, the method suffers from a **prototype bias issue**, because the scarce labeled samples cannot provide a reliable mean estimation for the prototypes [25]. To address the drawback, some studies attempt to learn a one-step prototype rectification function from a large set of few-shot tasks [25, 41, 44]. However, characterizing the bias with a one-step function is too coarse to obtain an accurate prototype (as we will see in Table 3 of Section 4.4).

Instead of learning a one-step rectification function, we regard the bias reduction as a prototype optimization process and attempt to model it as continuous dynamics in this paper. In particular, the mean-based prototypes offered by pre-trained feature extractors are treated as the initial solutions of the prototype optimization, and then a Neural Ordinary Differential Equation (Neural ODE) [7] is leveraged to model the optimization dynamics. The special modeling scheme is inspired by the fact that the conventional Gradient Descent Optimization (GDO) formula is indeed an Euler-based discrete instantiation of an ODE [5]. Hence, we introduce a Neural ODE to learn the continuous optimization dynamics in base classes and apply this meta-knowledge on novel classes to obtain more reliable prototypes.

Based on the notion, we propose a novel prototype optimization based meta-learning framework, called MetaNODE. Specifically, we first pre-train a classifier on all base classes to obtain a feature extractor. Then, given a few-shot task, we average the extracted features of all labeled samples as the initial prototype for each class. As a sequel, these prototypes will be further optimized to reduce the prototype

bias. Even though the existing optimization based meta-learning methods (meta-optimizer) [3, 30, 32] can be utilized for this purpose, they all suffer from a common drawback, called **gradient bias issue**. The issue appears because all the existing meta-optimizers carefully model the hyper-parameters (e.g., initialization [30] and regularization parameters [3, 15]) in GDO as meta-knowledge, but roughly estimate the gradient in an average manner with very few samples, which is obviously inaccurate. Given that the gradient estimation is very biased, more accurate hyperparameters are not meaningful and cannot lead to a reliable prototype optimization. Hence, we design a novel Neural ODE based meta-optimizer by treating the gradient itself as meta-knowledge. In the meta-optimizer, a gradient flow inference network is designed, which learns to estimate the continuous gradients for prototype dynamics. Finally, the optimal prototypes can be obtained by solving the Neural ODE with a Runge-Kutta solver [2], and then the few-shot classification is performed with the obtained optimal prototypes. Our main contributions can be summarized as follows:

- We propose a novel prototype optimization based meta-learning framework to address the prototype bias issue, and at the same time identify a crucial problem of existing meta-optimizer, i.e., gradient bias issue.
- To address the issue, we propose a Neural ODE-based meta-optimizer by modeling the prototype evolution as a Neural ODE, which offers our framework the excellent ability to learn to optimize prototypes. Moreover, our framework can work in both inductive and transductive FSL settings.
- We conduct comprehensive experiments on miniImagenet, tieredImageNet, and CUB-200-2011. The results show that our method obtains superior performance over the previous state-of-the-art approaches.

## 2. Related Work

### 2.1. Inductive Few-Shot Learning

Inductive FSL assumes that information from test data cannot be utilized when classifying the novel classes samples. Recently, many methods have been developed, which can be roughly grouped into three categories. **1) Metric-based approaches.** This line of works focuses on learning a task-agnostic metric space and then predicting classes by a nearest-centroid classifier with Euclidean or cosine distance [18, 16, 22, 27, 37]. For example, Li et al. [22] proposed a category traversal module to find task-relevant features, aiming to classify each sample in a low-dimension and compact metric space. **2) Optimization-based approaches.** The key idea is to model the optimization algorithm over few labeled samples within a meta-learning framework

[15, 20, 31, 35], which is known as the meta-optimizer. For example, MAML [14], MetaLSTM [32], and ALFA [3] introduced meta-learners to learn to design initialization, update rule, and weight decay of optimization algorithm, respectively. **3) Pre-training based approaches.** This type of works mainly utilize a two-phases training manner to quickly adapt to novel tasks [13, 24, 29, 38, 43, 45, 46], i.e., pre-training and fine-tuning phases. For instance, Chen et al. [9] proposed to train a feature extractor from the entire base classes and then classify novel classes via a nearest neighbor classifier with cosine distance for few-shot tasks, which suffers from the prototype bias issue. In this paper: 1) we focus on the prototype bias issue and attempt to address it in an optimization-based manner; 2) we design a novel continuous meta-optimizer by regarding the gradient itself as meta-knowledge for prototype optimization.

### 2.2. Transductive Few-Shot Learning

Different from inductive FSL, transductive FSL assumes that all the test data can be accessed to make predictions for novel classes. Recently, transductive FSL techniques attract considerable attention, which can be divided into two categories. **1) Graph-based approaches.** This group of methods attempt to propagate the labels from labeled samples to unlabeled samples by constructing instance graphs [26, 42] for each FSL task. For instance, in [42], a distribution propagation graph network was devised for FSL, which explores distribution-level relations for label propagations. **2) Pre-training based approaches.** This kind of studies still focuses on the two-stages training paradigms [11, 1]. Different from inductive FSL methods, these methods further explore the unlabeled samples to train a better classifier [4, 19, 40, 48] or construct a more reliable prototype [25, 41, 44]. For example, Liu et al. [25] proposed a label propagation and a feature shifting strategy for more reliable prototype estimation. In this paper, we also target at obtaining a reliable prototype. Different from these existing methods, we regard it as an optimization problem and propose a new meta-optimizer to solve it. Besides, our method is more flexible, which can be applied to both transductive and inductive FSL settings.

### 2.3. Neural ODE

Neural ODE, proposed by [7], is a continuous-time model, aiming to capture the evolution process of a state by representing its gradient flow with a neural network. Recently, it has been successfully used in various domains, such as irregular time series prediction [34], knowledge graph forecasting [12], MRI image reconstruction [6], image dehazing [36]. However, to our best knowledge, there is no previous work to explore it for the FSL problem. In this paper, we propose a novel Neural ODE-based meta-optimizer to fill this gap. Its advantage is that the prototype

evolution dynamics can be captured in a continuous manner, which produces more accurate prototypes for FSL.

### 3. Methodology

#### 3.1. Problem Definition

For a  $N$ -way  $K$ -shot the problem, two datasets are given: a base class dataset  $\mathcal{D}_{base}$  and a novel class dataset  $\mathcal{D}_{novel}$ . The base class dataset  $\mathcal{D}_{base} = \{(x_i, y_i)\}_{i=0}^B$  is made up of abundant labeled samples, where each sample  $x_i$  is labeled with a base class  $y_i \in \mathcal{C}_{base}$  ( $\mathcal{C}_{base}$  denotes the set of base classes). The novel class dataset consists of two subsets: a training set  $\mathcal{S}$  with few labeled samples (called support set) and a test set  $\mathcal{Q}$  consisting of unlabeled samples (called query set). Here, the support set  $\mathcal{S}$  is composed of  $N$  classes sampled from the set of novel class  $\mathcal{C}_{novel}$ , and each class only contains  $K$  labeled samples. Note that the base class set and novel class set are disjoint, i.e.,  $\mathcal{C}_{base} \cap \mathcal{C}_{novel} = \emptyset$ . Our goal is to learn a good classifier for query set  $\mathcal{Q}$  given the support set  $\mathcal{S}$  and the base class dataset  $\mathcal{D}_{base}$ .

#### 3.2. Closer Look at Optimization

Before introducing MetaNODE, we first revisit the Gradient Descent Optimization algorithm (GDO).

**Gradient Bias.** Formally, let  $L(p)$  be a differentiable loss function with prototype  $p$ , and  $\nabla L(p)$  be its gradient, i.e.,  $\nabla L(p) = \frac{\partial L(p)}{\partial p}$ . Following the standard way of GDO, the optimal prototype can be obtained by performing  $M$  iterations, given the initial prototype  $p_0$ . That is,

$$p_{t+1} = p_t - \eta \nabla L(p_t), \quad (1)$$

where  $t = 0, 1, \dots, M-1$  and  $\eta$  is a learning rate. The GDO has shown superior performance with sufficient samples. However, recent studies [32] show that it tends to be over-fitting in FSL, due to the data scarcity. To address the issue, a variety of methods extend GDO for FSL by learning its initialization [14, 30], update rule [32], learning rate [23], or weight decay [3]. In all these methods, the gradient  $\nabla L(p_t)$  is estimated in an average manner with very few labeled samples. That is,

$$\nabla L(p_t) = \frac{1}{|\mathcal{S}|} \sum_{(x_i, y_i) \in \mathcal{S}} \nabla L_{(x_i, y_i)}(p_t), \quad (2)$$

where  $|\cdot|$  denotes the size of a set and  $\nabla L_{(x_i, y_i)}(p_t)$  is the gradient of the sample  $(x_i, y_i) \in \mathcal{S}$ . Such estimation is obviously inaccurate in the few-shot scenarios, because the number of available labeled samples (e.g.,  $K=1$  or 5) is far less than the expected amount. As a result, the optimization performance of existing methods is limited. This is exactly the gradient bias issue mentioned in the introduction.

**A Dynamical View on Optimization.** Recent studies [5] found that the iteration process described in Eq. 1 can be

viewed as an Euler discretization of an ordinary differential equation (ODE). That is,

$$\frac{dp(t)}{dt} = -\nabla L(p(t), t), \quad (3)$$

where  $\frac{dp(t)}{dt}$  is referred to as a continuous-time gradient flow of prototype  $p(t)$ . Note that, different from Eq. 1, the prototype becomes a continuous-time variable, instead of a discrete sequence, thus we denote it as  $p(t)$ . Inspired by this fact, we regard the prototype optimization problem as an initial value problem to an ODE, where the initial and final state is the initial and optimal prototype, respectively.

To diminish the gradient bias of Eq. 2, we propose a Gradient Flow Inference Network (GradNet)  $f_{\theta_o}()$  with parameters  $\theta_o$  (described in Section 3.4) as a meta-learner to learn to infer its gradient flow, and then the ODE turns into a Neural ODE, i.e.,  $\frac{dp(t)}{dt} = f_{\theta_o}(p(t), t)$ . Hence, the process of prototype optimization can be described as: given the initial prototype  $p(0)$  as the initial condition at  $t = 0$ , and the GradNet  $f_{\theta_o}()$ , the optimal prototype can be solved by evaluating the Neural ODE at the last time point  $t = M$ , i.e.,  $p(M) = p(0) + \int_{t=0}^M f_{\theta_o}(p(t), t)$ , where the integral term can be calculated by an ODE solver. That is,

$$p(M) = ODESolve(f_{\theta_o}, p(0), M), \quad (4)$$

where  $ODESolve()$  denotes an ODE solver, e.g., Runge-Kutta method [2]. We term the Neural ODE based optimization method as Neural ODE-based meta-optimizer. The advantage of this meta-optimizer is that the prototype evolution dynamics can be captured in a continuous manner, which produces more accurate prototypes for FSL.

#### 3.3. MetaNODE Framework

In this section, we introduce how to train and leverage the Neural ODE-based meta-optimizer to address FSL problem. As shown in Figure 1, the MetaNODE framework consists of three phases, i.e., pre-training, meta-training, and meta-test. Next, we elaborate on them, respectively.

**Pre-Training.** Following [33], we first construct a convolution neural network (CNN) based model, which is made up of a feature extractor, a linear category classifier and a linear rotation classifier. Then, we train this model with the base classes by minimizing two cross-entropy losses, i.e., a standard classification loss  $L_{ce}$  and an auxiliary rotation loss  $L_{ro}$ , aiming to obtain rotation-invariant image representations. Finally, we can obtain a feature extractor  $f_{\theta_f}()$  with parameters  $\theta_f$ , which will be frozen in the following phases.

**Meta-Training.** Upon the feature extractor  $f_{\theta_f}()$ , we employ a nearest neighbor classifier for each few-shot task by following [9]. Here, its prototype is obtained by two stages: 1) initializing it by averaging the features of few labeled samples; and 2) further optimizing it by leveraging

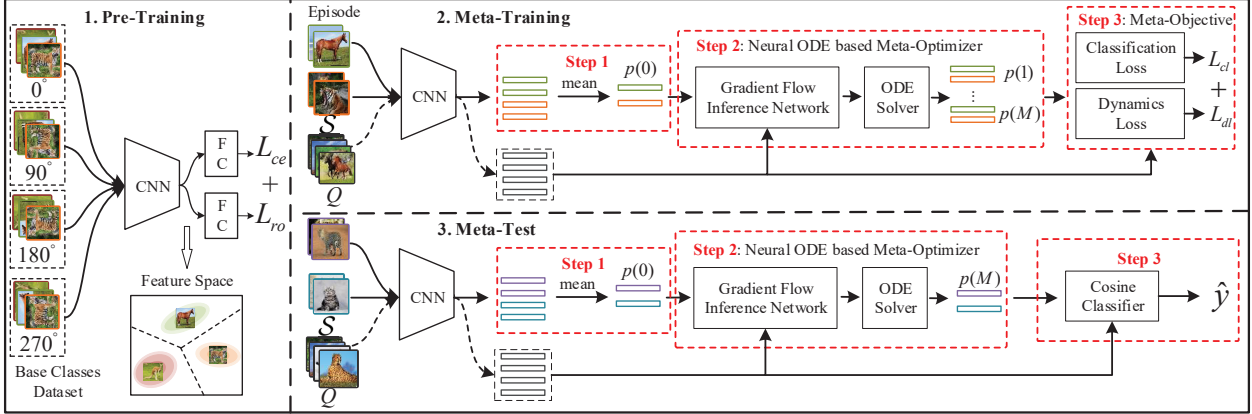


Figure 1. The overall framework of MetaNODE, which incorporates a Neural ODE to model the prototype optimization dynamics.

the Neural ODE-based meta-optimizer. Next, we elaborate on how to train our meta-optimizer to optimize prototype in an episodic training manner [14].

As shown in Figure 1, we first construct a number of  $N$ -way  $K$ -shot tasks (called episodes) from base class dataset  $\mathcal{D}_{base}$ . For each episode, we randomly sample  $N$  classes from base classes  $\mathcal{C}_{base}$ ,  $K$  images for each class as support set  $S$ , and  $M$  images for each class as query set  $Q$ . After that in each episode, we take the following three steps to train our meta-optimizer.

**Step 1.** We average the features of all labeled samples of class  $k$  as its initial prototype  $p_k(0)$ . That is,

$$p_k(0) = \frac{1}{|\mathcal{S}_k|} \sum_{(x_i, y_i) \in \mathcal{S}_k} f_{\theta_f}(x_i), \quad (5)$$

where  $\mathcal{S}_k$  denotes the support set extracted from class  $k$ . Besides, we denote the prototype set  $\{p_k(t)\}_{k=0}^{N-1}$  as the prototype  $p(t)$  of classifiers at time  $t$ , i.e.,  $p(t) = \{p_k(t)\}_{k=0}^{N-1}$ .

**Step 2:** To eliminate the estimation bias of Eq. 5, we first regard  $p(0)$  (i.e.,  $t = 0$ ) as an initial condition, and view the process of prototype evolution as a continuous-time dynamics. Then, a Neural ODE-based meta-optimizer is designed to model this dynamics, which consists of a gradient flow inference network (GradNet) and an ODE solver. Here, the former one aims to infer the gradient flow of prototype dynamics, which is implemented by a neural network  $f_{\theta_o}(\cdot)$  with parameter  $\theta_o$  (Please refer to Section 3.4 for more details). The latter accounts for solving the Neural ODE to obtain the optimal prototype, such as the Runge-Kutta method [2]. Finally, the prototype  $p(t)$  can be expressed as a Neural ODE, i.e.,  $\frac{dp(t)}{dt} = f_{\theta_o}(p(t), t)$  and the prototype evolution path can be obtained by solving the Neural ODE at  $t = 1, 2, \dots, M$ , respectively. That is,

$$p(1), \dots, p(M) = ODEsolve(f_{\theta_o}, p(0), (1, \dots, M)), \quad (6)$$

where  $M$  denotes the integral time. We empirically find that the Neural ODE can converge when  $M$  is set as 25.

**Step 3:** To effectively learn the dynamics, we propose a novel optimization-path based meta-objective, which consists of classification loss  $L_{cl}$  and dynamics loss  $L_{dl}$ . The classification loss  $L_{cl}$  aims to learn an optimal prototype to classify each query sample  $x_i \in \mathcal{Q}$ . Specifically, we regard the prototype  $p(M)$  at time  $t = M$  as the optimal prototype and then evaluate class probability by calculating the cosine similarity between  $p(M)$  and each sample  $f_{\theta_f}(x_i)$ . That is,

$$P(y = k | x_i, \mathcal{S}, \theta_f, \theta_o) = \frac{e^{<f_{\theta_f}(x_i), p_k(M)> \cdot \gamma}}{\sum_c e^{<f_{\theta_f}(x_i), p_c(M)> \cdot \gamma}}, \quad (7)$$

where  $< \cdot >$  denote the cosine similarity of two vectors, and  $\gamma$  is a scale parameter. Following [8],  $\gamma = 10$  is used. Finally, the classification loss  $L_{cl}$  is defined as the mean negative log-likelihood of all query samples, that is,

$$L_{cl} = \frac{1}{|\mathcal{Q}|} \sum_{(x_i, y_i) \in \mathcal{Q}} -\log(P(y_i | x_i, \mathcal{S}, \theta_f, \theta_o)). \quad (8)$$

The dynamics loss  $L_{dl}$  accounts for constraining the Neural ODE to fit the prototype evolution path. Specifically, given the initial prototype (i.e.,  $p'(0) = p(0)$ ) and the label  $y_i$  of each query sample  $x_i \in \mathcal{Q}$ , we can obtain the ground truth of prototype evolution path by performing  $M$ -steps GDO algorithm to maximize the likelihood estimation of each sample  $(x_i, y_i) \in \mathcal{S} \cup \mathcal{Q}$ . That is,

$$\max_{p'(t)} \sum_{(x_i, y_i) \in \mathcal{S} \cup \mathcal{Q}} \log\left(\frac{e^{<f_{\theta_f}(x_i), p'_{y_i}(t)> \cdot \gamma}}{\sum_c e^{<f_{\theta_f}(x_i), p'_c(t)> \cdot \gamma}}\right), \quad (9)$$

where the obtained prototypes at  $t = 1, 2, \dots, M$  is regarded as the ground truth of prototype evolution path, i.e.,  $\{p'(1), p'(2), \dots, p'(M)\}$ . Thus, the dynamics loss  $L_{dl}$  can be defined as their Mean-Square Error (MSE) between  $\{p'(1), p'(2), \dots, p'(M)\}$  and  $\{p(1), p(2), \dots, p(M)\}$ :

$$L_{dl} = \frac{1}{NM} \sum_{k=0}^{N-1} \sum_{t=1}^{M-1} MSE(p_k(t), p'_k(t)), \quad (10)$$

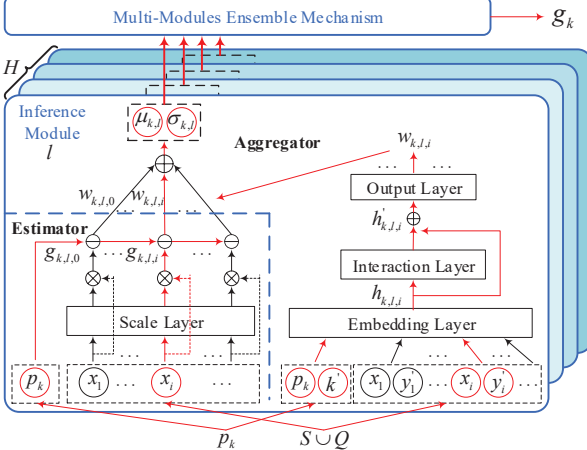


Figure 2. Illustration of the gradient flow inference network.

where  $MSE(\cdot)$  denotes a MSE loss between two vectors.

Finally, we train our meta-optimizer by minimizing the two loss functions defined in Eqs. 8 and 10. That is,

$$\min_{\theta_o} \mathbb{E}_{(\mathcal{S}, \mathcal{Q}) \in \mathbb{T}} L_{cl} + \lambda L_{dl}, \quad (11)$$

where  $\mathbb{T}$  denotes the set of  $N$ -way  $K$ -shot tasks, and  $\lambda$  is a hyperparameter adjusting classification loss  $L_{cl}$  and dynamics loss  $L_{dl}$ . In this paper,  $\lambda = 1$  is used.

**Meta-Test.** Its workflow is similar to the Meta-Training phase. The key difference is that we remove the loss evaluation defined in Eqs. 8 ~ 11 and directly perform few-shot classification for novel classes by following Eqs. 5 ~ 7.

### 3.4. Gradient Flow Inference Network

In this section, we elaborate on the details of GradNet  $f_{\theta_o}(\cdot)$  used in MetaNODE. Our notion is treating the support set  $\mathcal{S}$ , query set  $\mathcal{Q}$ , and prototype  $p(t) = \{p_k(t)\}_{k=0}^{N-1}$  as inputs and the estimated gradient flow  $g(t) = \{g_k(t)\}_{k=0}^{N-1}$  as outputs, and then building a gradient flow inference network with multi-modules ensemble mechanism, as shown in Figure 2. Instead of performing a single inference module, we design multiple inference modules with the same structure to estimate  $g(t)$ . Here, each inference module consists of an estimator and an aggregator. The estimator aims to predict the contributed gradient by each sample  $(x_i, y_i) \in \mathcal{S} \cup \mathcal{Q}$ . The aggregator accounts for evaluating the contribution of each sample and then combining estimated gradients with a weighted mean. For clarity, we omit the symbol  $t$  and take inference module  $l$  and class  $k$  as an example to detail them.

**Estimator.** As we adopt the cosine-based classifier, the prototype is expected to approach the angle center of all the samples in each class. To eliminate the impact of vector norm, we first employ a scale layer  $f_{\theta_{os}^l}(\cdot)$  with parameters  $\theta_{os}^l$  to transform the features of each sample  $(x_i, y_i)$  to an appropriate scale and obtain a scaled feature by an element-wise product. Then, we estimate the gradient flow  $g_{k,l,i}$  by

calculating the difference vector between the scaled features and the prototype  $p_k$ . That is,

$$g_{k,l,i} = f_{\theta_f}(x_i) \otimes f_{\theta_{os}^l}(f_{\theta_f}(x_i) \| p_k) - p_k, \quad (12)$$

where  $\|$  is a concatenation operation of two vectors and  $\otimes$  denotes an element-wise product operation.

**Aggregator.** Based on the estimated gradient flow  $g_{k,l,i}$  contributed by each sample  $(x_i, y_i)$ , we discuss how to combine them. Intuitively, different samples make varying contributions to the gradient flow prediction of prototype  $p_k$ . To this end, we design an aggregator to predict their weights, which consists of an embedding layer  $f_{\theta_{oe}^l}(\cdot)$ , an interaction layer  $f_{\theta_{oi}^l}(\cdot)$ , and an output layer  $f_{\theta_{oo}^l}(\cdot)$ , where  $\theta_{oe}^l$ ,  $\theta_{oi}^l$ , and  $\theta_{oo}^l$  denote their parameters, respectively. Next, we detail the three components, respectively.

**1) Embedding Layer.** We first fuse their features by calculating the element-wise product of  $p_k$  and  $f_{\theta_f}(x_i)$ . Then, these features and their one-hot vector transformed by their labels  $k$  and  $y_i$  (Note that we replace the one-hot vector of unlabeled samples by a  $N$ -dim vector with value of  $1/N$ ) are concatenated as inputs of the embedding layer  $f_{\theta_{oe}^l}(\cdot)$ . As a result, the embedding  $h_{k,l,i}$  can be obtained:

$$h_{k,l,i} = f_{\theta_{oe}^l}(k' \| p_k \| y_i' \| f_{\theta_f}(x_i) \| p_k \otimes f_{\theta_f}(x_i)), \quad (13)$$

where  $k'$  and  $y_i'$  denote the one-hot vector of labels  $k$  and  $y_i$ , respectively; and  $\|$  is a concatenation operation.

**2) Interaction Layer.** As the representation  $h_{k,l,i}$  delivered by Eq. 13 does not exploit the correlation between samples, we introduce an interaction layer here to model this. Based on the embedding  $h_{k,l,i}$ , we employ a multi-head based attention mechanism [39] to model the relationships among these sample pairs. As a result, an enhanced embedding  $h'_{k,l,i}$  can be obtained:

$$h'_{k,l,i} = f_{\theta_{oi}^l}(\{h_{k,l,i}\}_{i=0}^{|\mathcal{S} \cup \mathcal{Q}|-1}) + h_{k,l,i}, \quad (14)$$

where we note that a residual connection is also introduced, which can provide more robust representations.

**3) Output Layer.** We first regard the enhanced embedding  $h'_{k,l,i}$  as inputs of the output layer  $f_{\theta_{oo}^l}(\cdot)$  to predict the weight  $\alpha_{k,l,i}$  of each sample  $x_i$ , that is,  $\alpha_{k,l,i} = f_{\theta_{oo}^l}(h'_{k,l,i})$ . Then, a softmax function and a normalization function are used to obtain the normalized weight  $w_{k,l,i}$ :

$$w_{k,l,i} = \frac{e^{\alpha_{k,l,i}}}{\sum_c e^{\alpha_{c,l,i}}} / \sum_{i=0}^{|\mathcal{S} \cup \mathcal{Q}|-1} \frac{e^{\alpha_{k,l,i}}}{\sum_c e^{\alpha_{c,l,i}}}. \quad (15)$$

Finally, we apply the weight  $w_{k,l,i}$  to integrate the estimated gradient  $g_{k,l,i}$ , and then obtain the aggregated gradient  $\mu_{k,l}$  and its variance  $\sigma_{k,l}^2$ :

$$\mu_{k,l} = \sum_i w_{k,l,i} g_{k,l,i}, \quad \sigma_{k,l}^2 = \sum_i w_{k,l,i} (g_{k,l,i} - \mu_{k,l})^2, \quad (16)$$

where  $\mu_{k,l}$  is the gradient estimated by module  $l$  for class  $k$ . **Multi-Modules Ensemble Mechanism.** In this part, we discuss how to combine these gradients  $\{\mu_{k,l}\}_{l=0}^{H-1}$  estimated by all inference modules by leveraging their variances  $\{\sigma_{k,l}^2\}_{l=0}^{H-1}$ , where  $H$  denotes the number of inference modules. Intuitively, the variance reflects the inconsistency of gradients contributed by all samples, i.e., the larger variance implies greater uncertainty. Hence, to obtain a more reliable gradient flow, we regard the variances as weights to combine these gradients. That is, the gradients with small variances are allocated with large weights as:

$$g_k = \beta \left[ \sum_{l=0}^{H-1} (\sigma_{k,l}^2)^{-1} \right]^{-1} \left[ \sum_{l=0}^{H-1} (\sigma_{k,l}^2)^{-1} \mu_{k,l} \right], \quad (17)$$

where  $g_k$  denotes the estimated gradient flow for prototype  $p_k$ , and  $\beta$  denotes a term of exponential decay with time  $t$ , i.e.,  $\beta = \beta_0 \xi^{-\frac{t}{M}}$  ( $\beta_0$  and  $\xi$  are hyperparameters, which are set as 0.2 and 0.5, respectively). In the above process, the samples of both query set  $\mathcal{Q}$  and support set  $\mathcal{S}$  are utilized to learn the gradient flow. Thus, it can be regarded as a transductive FSL method.

For inductive FSL, the inference workflow is similar to the above process defined in Eqs. 12 ~ 17. The only difference is that the query set  $\mathcal{Q}$  is removed, and only support set  $\mathcal{S}$  and prototypes  $p(t)$  are given as inputs of the GradNet to estimate the gradient flow  $g_k$  for prototype  $p_k$ .

## 4. Performance Evaluation

### 4.1. Datasets and Settings

**MiniImagenet.** The dataset is derived from ImageNet dataset. It consists of 100 classes, where each class contains 600 images. Following the standard split in [9], we split the data set into 64 classes, 16 classes, and 20 classes for training, validation, and test, respectively.

**TieredImageNet.** The dataset is a larger dataset with 608 classes derived from ImageNet, where each class contains 1200 images. Following [9], the dataset is split into 20 high-level semantic categories for training, 6 high-level semantic categories for validation, and 8 high-level semantic categories for testing, respectively.

**CUB-200-2011.** The dataset is a fine-grained bird recognition dataset with 200 classes. It contains about 11,788 images. Following the standard split in [8], we split the data set into 100 classes, 50 classes, and 50 classes for training, validation, and testing, respectively.

### 4.2. Implementation Details

**Network Details.** We use ResNet12 [9] as the feature extractor. In our meta-optimizer, we use 4 inference modules to estimate the gradient flow. For each module, we use a two-layer MLP with 512-dimensional hidden layer for the

scale layer, a single-layers perceptron with 512-dimensional outputs for the the embedding layer, a multi-head attention module with 8 heads and each head contains 16 units for the interaction layer, and a single-layers perceptron for the output layer. ELU [10] is used as the activation function.

**Training details.** Following [9], we use an SGD optimizer to train the feature extractor for 100 epochs. In the meta-training phase, we train the Neural ODE-based meta-optimizer 50 epochs using Adam with a learning rate of 0.001 and a weight decay of 0.0005, where the learning rate is decayed by 0.1 at epochs 15, 30, and 40, respectively.

**Evaluation.** Following [9], we evaluate MetaNODE on 600 randomly sampled episodes (5-way 1-shot/5-shot setting) from the novel classes and report the mean accuracy together with the 95% confidence interval.

### 4.3. Experimental Results

We evaluate MetaNODE and various state-of-the-art approaches on general and fine-grained few-shot tasks.

**General Few-Shot Image Recognition.** Table 1 shows the results of various evaluated methods on miniImagenet and tieredImageNet. Compared with state-of-the-art methods, MetaNODE consistently achieves the best performance on both datasets. This demonstrates the superiority of MetaNODE. In inductive FSL setting, MetaNODE outperforms state-of-the-art methods, especially on 1-shot tasks by 2% ~ 4%. Specifically, compared with the best results of metric-based methods (RestoreNEt, CTM, and CAN), MetaNODE can achieve 1% ~ 4% higher accuracy. Different from these methods, we introduce a pre-training phase to learn image representation and a new meta-optimizer to polish the prototypes. The optimization-based methods also focus on modeling optimization algorithm over few labeled samples in a meta-learning manner. However, different from them: 1) we regard the gradient flow as meta-knowledge; and 2) we focus on optimizing prototypes instead of the entire model. The result validates the superiority of our approach. Finally, compared with the pre-training based methods, our method exceeds these methods by 1% ~ 4%. The main reason is that we diminish the prototype bias by introducing a meta-optimizer to polish prototypes.

In transductive FSL setting, it can also be found that MetaNODE outperforms state-of-the-art methods (e.g., TIM-GD and BD-CSPN), around 1% ~ 5%. Specifically, different from these graph and pre-training based methods, our method utilizes the unlabeled samples to infer the gradient flow of prototype evolution, instead of to boost image representation or as a regularization of training classifier. It's worth noting that our method also beats BD-CSPN, SRestoreNet, and SIB, which also attempt to obtain more representative prototypes. Different from them, we focus on modeling the prototype dynamics, instead of restoring prototype or inferring the loss of unlabeled samples.

Table 1. Experiment results on miniImageNet and tieredImageNet. The best results are highlighted in bold.

Setting	Method	Type	Backbone	miniImagenet		tieredImageNet	
				5-way 1-shot	5-way 5-shot	5-way 1-shot	5-way 5-shot
In ductive	RestoreNet [41]	Metric	ResNet12	59.28 $\pm$ 0.20%	– $\pm$ –%	– $\pm$ –%	– $\pm$ –%
	CTM [22]	Metric	ResNet12	62.05 $\pm$ 0.55%	78.63 $\pm$ 0.06%	64.78 $\pm$ 0.11%	81.05 $\pm$ 0.52%
	CAN [18]	Metric	ResNet12	63.85 $\pm$ 0.48%	79.44 $\pm$ 0.34%	69.89 $\pm$ 0.51%	84.23 $\pm$ 0.37%
	MetaLSTM [32]	Optimization	Conv4	43.44 $\pm$ 0.77%	60.60 $\pm$ 0.71%	– $\pm$ –%	– $\pm$ –%
	MAML [14]	Optimization	ResNet12	58.37 $\pm$ 0.49%	69.76 $\pm$ 0.46%	58.58 $\pm$ 0.49%	71.24 $\pm$ 0.43%
	Warp-MAML [15]	Optimization	Conv4	52.3 $\pm$ 0.8%	68.4 $\pm$ 0.6%	57.2 $\pm$ 0.9%	71.4 $\pm$ 0.7%
	ALFA [3]	Optimization	ResNet12	59.74 $\pm$ 0.49%	77.96 $\pm$ 0.41%	64.62 $\pm$ 0.49%	82.48 $\pm$ 0.38%
	NewBaseline [9]	Pre-training	ResNet12	63.17 $\pm$ 0.23%	79.26 $\pm$ 0.17%	68.62 $\pm$ 0.27%	83.29 $\pm$ 0.18%
	Neg-Cosine [24]	Pre-training	ResNet12	63.85 $\pm$ 0.81%	81.57 $\pm$ 0.56%	– $\pm$ –%	– $\pm$ –%
	CentAlign [24]	Pre-training	ResNet18	59.88 $\pm$ 0.67%	80.35 $\pm$ 0.73%	69.29 $\pm$ 0.56%	85.97 $\pm$ 0.49%
Trans ductive	Baseline++ [8]	Pre-training	ResNet18	51.87 $\pm$ 0.77%	75.68 $\pm$ 0.63%	– $\pm$ –%	– $\pm$ –%
	MetaNODE	Pre-training	ResNet12	<b>66.52 <math>\pm</math> 0.88%</b>	<b>81.94 <math>\pm</math> 0.55%</b>	<b>72.88 <math>\pm</math> 0.91%</b>	<b>84.94 <math>\pm</math> 0.70%</b>
	DPGN [42]	Graph	ResNet12	67.77 $\pm$ 0.32%	84.60 $\pm$ 0.43%	72.45 $\pm$ 0.51%	87.24 $\pm$ 0.39%
	EPNet [33]	Graph	ResNet12	66.50 $\pm$ 0.89%	81.06 $\pm$ 0.60%	76.53 $\pm$ 0.87%	87.32 $\pm$ 0.64%
	ICI [40]	Pre-training	ResNet12	65.77 $\pm$ –%	78.94 $\pm$ –%	80.56 $\pm$ –%	87.93 $\pm$ –%
	TIM-GD [4]	Pre-training	ResNet18	73.9 $\pm$ –%	85.0 $\pm$ –%	79.9 $\pm$ –%	88.5 $\pm$ –%
	LaplacianShot [48]	Pre-training	ResNet18	72.11 $\pm$ 0.19%	82.31 $\pm$ 0.14%	78.98 $\pm$ 0.21%	86.39 $\pm$ 0.16%
	BD-CSPN [25]	Pre-training	WRN-28-10	70.31 $\pm$ 0.93%	81.89 $\pm$ 0.60%	78.74 $\pm$ 0.95%	86.92 $\pm$ 0.63%
	SRestoreNet [41]	Pre-training	ResNet18	61.14 $\pm$ 0.22%	– $\pm$ –%	– $\pm$ –%	– $\pm$ –%
	SIB [19]	Pre-training	WRN-28-10	70.0 $\pm$ 0.6%	79.2 $\pm$ 0.4%	– $\pm$ –%	– $\pm$ –%
	MetaNODE	Pre-training	ResNet12	<b>77.46 <math>\pm</math> 0.98%</b>	<b>85.12 <math>\pm</math> 0.61%</b>	<b>84.08 <math>\pm</math> 0.94%</b>	<b>87.98 <math>\pm</math> 0.64%</b>

Table 2. Experiment results on CUB-200-2011.

Setting	Method	CUB-200-2011	
		5-way 1-shot	5-way 5-shot
In ductive	RestoreNet [41]	74.32 $\pm$ 0.91%	– $\pm$ –%
	MAML [14]	55.92 $\pm$ 0.95%	72.09 $\pm$ 0.76%
	Neg-Cosine [24]	72.66 $\pm$ 0.85%	89.40 $\pm$ 0.43%
	CentAlign [24]	74.22 $\pm$ 1.09%	88.65 $\pm$ 0.55%
	Baseline++ [8]	67.02 $\pm$ 0.90%	83.58 $\pm$ 0.54%
	MetaNODE	<b>80.45 <math>\pm</math> 0.74%</b>	<b>91.80 <math>\pm</math> 0.40%</b>
Trans ductive	DPGN [42]	75.71 $\pm$ 0.47%	91.48 $\pm$ 0.33%
	EPNet [33]	82.85 $\pm$ 0.81%	91.32 $\pm$ 0.41%
	ICI [40]	87.87%	92.38%
	TIM-GD [4]	82.2 $\pm$ –%	90.8 $\pm$ –%
	LaplacianShot [48]	80.96%	88.68%
	BD-CSPN [25]	87.45%	91.74%
	RestoreNet [41]	76.85 $\pm$ 0.95%	– $\pm$ –%
	MetaNODE	<b>91.33 <math>\pm</math> 0.74%</b>	<b>93.48 <math>\pm</math> 0.37%</b>

**Fine-Grained Few-Shot Image Recognition.** The results on CUB-200-2011 are shown in Table 2. Similar to Table 1, we observe that MetaNODE significantly outperforms the state-of-the-art methods, achieving 2%  $\sim$  6% higher accuracy scores. This further verifies the effectiveness of MetaNODE in the fine-grained FSL task, which exhibits smaller class differences than the general FSL task.

#### 4.4. Statistical Analysis

**Does MetaNODE eliminate prototype bias?** In Table 3, we report the cosine similarity between the initial (optimal) prototypes, i.e.,  $p(0)$  ( $p(M)$ ) and the corresponding class center on 5-way 1-shot tasks of miniImagenet. Note that

the class center is obtained by averaging the features of all labeled and unlabeled samples. The reported results are averaged on 1000 episodes. We select BD-CSPN and SRestoreNet as the baselines because they also attempt to reduce prototype bias. The results show that MetaNODE obtains more accurate prototypes than them, which is because MetaNODE regards it as a prototype optimization problem, and solves it from the view of continuous dynamics.

**Does MetaNODE eliminate gradient bias?** In Table 4, we randomly select 1000 episodes from miniImageNet, and then calculate the cosine similarity between the averaged (inferred) and the real gradient. Here, the averaged gradient is obtained by Eq. 2 and the inferred gradient is estimated by the proposed GradNet. Besides, the real gradient is estimated by using all labeled and unlabeled samples by following Eq. 2. We select SIB as the baseline, which estimates the gradient by inferring the loss value of unlabeled samples. It can be observed that MetaNODE can achieve higher cosine similarities than SIB, which implies that MetaNODE obtains more accurate gradient estimation. This is because: 1) MetaNODE models the gradient flow from the dynamics view; and 2) an optimization path-based meta-objective is designed to capture the prototype dynamics.

**Can our meta-optimizer converge?** In Figure 3(a), we randomly select 1000 episodes from miniImageNet, and then report their test accuracy and loss from integral time  $t = 1$  to 30. It can be observed that our meta-optimizer can converge to a stable result when  $t = 25$ . Hence,  $M = 25$  is a default setting in our approach.

**How our meta-optimizer works?** We visualize the proto-

Table 3. Experiments of prototype bias on miniImagenet.

Methods	Initial Prototypes	Optimal Prototypes
BD-CSPN [25]	0.64	0.75
SRestoreNet [41]	0.64	0.85
MetaNODE	0.64	0.94

Table 4. Experiments of gradient bias on miniImagenet.

Methods	Averaged Gradient	Infered Gradient
SIB [19]	0.0437	0.0659
MetaNODE	0.0437	0.1706

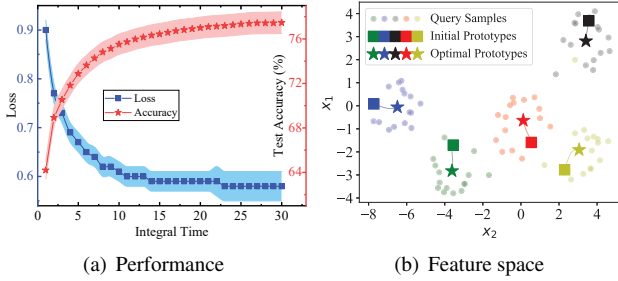


Figure 3. Visualization of prototypes dynamics on miniImagenet.

type dynamics of a 5-way 1-shot task on miniImagenet in the feature space, as shown in Figure 3(b). Note that since there is only one support sample in each class, its feature is used as the initial prototype. We find that the initial prototypes marked by squares flow to optimal prototypes marked by stars, much closer to the class centers. This visualization indicates that the meta-optimizer effectively learns the representative prototypes in the feature space.

#### 4.5. Ablation Study

**Is our meta-optimizer effective?** In Table 5, we conduct an ablation study to analyze the effectiveness of our meta-optimizer. Specifically, in inductive FSL setting, (i) we remove our meta-optimizer as a baseline, and then our model degenerates into the pre-training method with mean-based prototypes [9]; (ii) we remove the mean-based prototypes and add an ANIL-based meta-optimizer [30] on (i) to learn a good initial classifier; (iii) we add the MetaLSTM-based meta-optimizer [32] on (i) to optimize the prototypes; (iv) we replace MetaLSTM by the ALFA-based meta-optimizer [3] on (iii); (v) different from (iv), we replace MetaLSTM by our meta-optimizer, and then obtain MetaNODE; and (vi) we further explore unlabeled samples on (v). From the results of (i) ~ (v), we observe that: 1) the performance of (v) exceeds (i) around 2% ~ 5%, which means that it is helpful to leverage the optimization-based method to polish prototypes; 2) the performance of (v) exceeds (ii) ~ (iv) around 1% ~ 6%, which demonstrates the superiority of our meta-optimizer. This is because our meta-optimizer regards the gradient itself as meta-knowledge, instead of hy-

Table 5. Ablation study of meta-optimizer on miniImagenet. QS denotes unlabeled (query) samples from query set  $Q$ .

	Method	5-way 1-shot	5-way 5-shot
(i)	Baseline	61.22 $\pm$ 0.84%	78.72 $\pm$ 0.60%
(ii)	+ ANIL [30]	60.67 $\pm$ 0.81%	77.98 $\pm$ 0.59%
(iii)	+ MetaLSTM [32]	63.85 $\pm$ 0.81%	79.49 $\pm$ 0.65%
(iv)	+ ALFA [3]	64.37 $\pm$ 0.79%	80.75 $\pm$ 0.57%
(v)	+ Neural ODE	66.52 $\pm$ 0.88%	81.49 $\pm$ 0.55%
(vi)	+ Neural ODE + QS	77.46 $\pm$ 0.98%	85.12 $\pm$ 0.61%

Table 6. Ablation study of meta-objective on miniImagenet.

	Method	5-way 1-shot	5-way 5-shot
(i)	MetaNODE	77.46 $\pm$ 0.98%	85.12 $\pm$ 0.61%
(ii)	w/o $L_{cl}$	75.45 $\pm$ 1.07%	83.72 $\pm$ 0.55%
(iii)	w/o $L_{dl}$	75.92 $\pm$ 1.06%	83.85 $\pm$ 0.64%

Table 7. Ablation study of ensemble mechanism on miniImagenet.

	Method	5-way 1-shot	5-way 5-shot
(i)	w/ ensemble	77.46 $\pm$ 0.98%	85.12 $\pm$ 0.61%
(ii)	w/o ensemble	76.04 $\pm$ 0.93%	83.96 $\pm$ 0.57%

perparameters like weight decay [3]. Finally, comparing the results of (v) with (vi), we find that introducing unlabeled samples can significantly enhance our meta-optimizer.

**Is the meta-objective described in Eq. 11 effective?** In Table 6, we assess the effects of two losses, i.e.,  $L_{cl}$  and  $L_{dl}$ . Specifically, in meta-training phase: (i) we contain all meta-objectives to train our model; (ii) we remove  $L_{cl}$  on (i); and (iii) we remove  $L_{dl}$  on (i). It can be found that the classification accuracy of MetaNODE decreases by 1% ~ 2% when  $L_{cl}$  and  $L_{dl}$  are removed. This indicates that it is beneficial to jointly consider the two kinds of loss.

**Is the ensemble mechanism effective?** In Table 7, we evaluate the effect of ensemble mechanism. Specifically, (i) we use the mechanism on GradNet, i.e.,  $H = 4$ ; (ii) we remove it on (i), i.e.,  $H = 1$ . We find that the performance decreases by 1% ~ 2% when removing it. This result implies that employing multiple inference modules is beneficial. We note that when only using a single module, our model still achieves superior performance on 1-shot tasks.

## 5. Conclusion

In this paper, we explore the optimization-based meta-learning methods to diminish the prototype bias for few-shot learning, i.e., learning to optimize prototypes. We design a novel Neural ODE-based meta-optimizer and an optimization path-based meta-objective to learn to capture the continuous prototype dynamics. Experiments on three datasets show that our model significantly obtains superior performance over state-of-the-art methods. We also conduct extensive statistical experiments and ablation studies, which further verify the effectiveness of our method.

## References

- [1] Arman Afrasiyabi, Jean-François Lalonde, and Christian Gagné. Associative alignment for few-shot image classification. In *ECCV*, volume 12350, pages 18–35, 2020. [2](#)
- [2] Roger Alexander. Solving ordinary differential equations I: nonstiff problems (E. hairer, s. p. norsett, and g. wanner). *SIAM Rev.*, 32(3):485–486, 1990. [2, 3, 4](#)
- [3] Sungyong Baik, Myungsub Choi, Janghoon Choi, Heewon Kim, and Kyoung Mu Lee. Meta-learning with adaptive hyperparameters. In *NeurIPS*, 2020. [2, 3, 7, 8](#)
- [4] Malik Boudiaf, Imtiaz Masud Ziko, Jérôme Rony, José Dolz, Pablo Piantanida, and Ismail Ben Ayed. Transductive information maximization for few-shot learning. In *NeurIPS*, 2020. [2, 7](#)
- [5] Zhiqi Bu, Shiyun Xu, and Kan Chen. A dynamical view on optimization algorithms of overparameterized neural networks. *CoRR*, abs/2010.13165, 2020. [1, 3](#)
- [6] Eric Z. Chen, Terrence Chen, and Shanhui Sun. MRI image reconstruction via learning optimization using neural odes. In *MICCAI 2020*, volume 12262, pages 83–93, 2020. [2](#)
- [7] Tian Qi Chen, Yulia Rubanova, Jesse Bettencourt, and David Duvenaud. Neural ordinary differential equations. In *NeurIPS*, pages 6572–6583, 2018. [1, 2](#)
- [8] Wei-Yu Chen, Yen-Cheng Liu, Zsolt Kira, Yu-Chiang Frank Wang, and Jia-Bin Huang. A closer look at few-shot classification. In *ICLR*, 2019. [4, 6, 7](#)
- [9] Yinbo Chen, Xiaolong Wang, Zhuang Liu, Huijuan Xu, and Trevor Darrell. A new meta-baseline for few-shot learning. In *ICML*, 2020. [1, 2, 3, 6, 7, 8](#)
- [10] Djork-Arné Clevert, Thomas Unterthiner, and Sepp Hochreiter. Fast and accurate deep network learning by exponential linear units (elus). In *ICLR*, 2016. [6](#)
- [11] Guneet Singh Dhillon, Pratik Chaudhari, Avinash Ravichandran, and Stefano Soatto. A baseline for few-shot image classification. In *ICLR*. OpenReview.net, 2020. [2](#)
- [12] Zifeng Ding, Zhen Han, Yunpu Ma, and Volker Tresp. Temporal knowledge graph forecasting with neural ODE. *CoRR*, abs/2101.05151, 2021. [2](#)
- [13] Carl Doersch, Ankush Gupta, and Andrew Zisserman. Crosstransformers: spatially-aware few-shot transfer. In Hugo Larochelle, Marc’Aurelio Ranzato, Raia Hadsell, Maria-Florina Balcan, and Hsuan-Tien Lin, editors, *NeurIPS*, 2020. [2](#)
- [14] Chelsea Finn, Pieter Abbeel, and Sergey Levine. Model-agnostic meta-learning for fast adaptation of deep networks. In Doina Precup and Yee Whye Teh, editors, *ICML*, volume 70, pages 1126–1135, 2017. [2, 3, 4, 7](#)
- [15] Sebastian Flennerhag, Andrei A. Rusu, Razvan Pascanu, Francesco Visin, Hujun Yin, and Raia Hadsell. Meta-learning with warped gradient descent. In *ICLR*, 2020. [1, 2, 7](#)
- [16] Fusheng Hao, Fengxiang He, Jun Cheng, Lei Wang, Jianzhong Cao, and Dacheng Tao. Collect and select: Semantic alignment metric learning for few-shot learning. In *ICCV*, pages 8459–8468. IEEE, 2019. [2](#)
- [17] Kaiming He, Xiangyu Zhang, Shaoqing Ren, and Jian Sun. Deep residual learning for image recognition. In *CVPR*, pages 770–778. IEEE Computer Society, 2016. [1](#)
- [18] Ruibing Hou, Hong Chang, Bingpeng Ma, Shiguang Shan, and Xilin Chen. Cross attention network for few-shot classification. In *NeurIPS*, pages 4005–4016, 2019. [2, 7](#)
- [19] Shell Xu Hu, Pablo Garcia Moreno, Yang Xiao, Xi Shen, Guillaume Obozinski, Neil D. Lawrence, and Andreas C. Damianou. Empirical bayes transductive meta-learning with synthetic gradients. In *ICLR*, 2020. [2, 7, 8](#)
- [20] Muhammad Abdullah Jamal and Guo-Jun Qi. Task agnostic meta-learning for few-shot learning. In *CVPR*, pages 11719–11727, 2019. [2](#)
- [21] Aoxue Li, Tiange Luo, Tao Xiang, Weiran Huang, and Liwei Wang. Few-shot learning with global class representations. In *ICCV*, pages 9714–9723, 2019. [1](#)
- [22] Hongyang Li, David Eigen, Samuel Dodge, Matthew Zeiler, and Xiaogang Wang. Finding task-relevant features for few-shot learning by category traversal. In *CVPR*, pages 1–10, 2019. [1, 2, 7](#)
- [23] Zhenguo Li, Fengwei Zhou, Fei Chen, and Hang Li. Metasgd: Learning to learn quickly for few shot learning. *CoRR*, abs/1707.09835, 2017. [3](#)
- [24] Bin Liu, Yue Cao, Yutong Lin, Qi Li, Zheng Zhang, Ming-sheng Long, and Han Hu. Negative margin matters: Understanding margin in few-shot classification. In *ECCV*, pages 438–455, 2020. [2, 7](#)
- [25] Jinlu Liu, Liang Song, and Yongqiang Qin. Prototype rectification for few-shot learning. In *ECCV*, 2020. [1, 2, 7, 8](#)
- [26] Yanbin Liu, Juho Lee, Minseop Park, Saehoon Kim, Eunho Yang, Sung Ju Hwang, and Yi Yang. Learning to propagate labels: Transductive propagation network for few-shot learning. In *ICLR*, 2019. [2](#)
- [27] Van Nhan Nguyen, Sigurd Løkse, Kristoffer Wickstrøm, Michael Kampffmeyer, Davide Roverso, and Robert Jenssen. [2](#)
- [28] Viraj Prabhu, Anitha Kannan, Murali Ravuri, Manish Chaplain, David A. Sontag, and Xavier Amatriain. Few-shot learning for dermatological disease diagnosis. In *MLHC*, volume 106, pages 532–552, 2019. [1](#)
- [29] Limeng Qiao, Yemin Shi, Jia Li, Yonghong Tian, Tiejun Huang, and Yaowei Wang. Transductive episodic-wise adaptive metric for few-shot learning. In *ICCV*, pages 3602–3611. IEEE, 2019. [2](#)
- [30] Aniruddh Raghu, Maithra Raghu, Samy Bengio, and Oriol Vinyals. Rapid learning or feature reuse? towards understanding the effectiveness of MAML. In *ICLR*, 2020. [2, 3, 8](#)
- [31] Aravind Rajeswaran, Chelsea Finn, Sham M. Kakade, and Sergey Levine. Meta-learning with implicit gradients. In *NeurIPS*, pages 113–124, 2019. [2](#)
- [32] Sachin Ravi and Hugo Larochelle. Optimization as a model for few-shot learning. In *ICLR*, 2017. [2, 3, 7, 8](#)
- [33] Pau Rodríguez, Issam H. Laradji, Alexandre Drouin, and Alexandre Lacoste. Embedding propagation: Smoother manifold for few-shot classification. In *ECCV*, pages 121–138, 2020. [3, 7](#)

[34] Yulia Rubanova, Tian Qi Chen, and David Duvenaud. Latent ordinary differential equations for irregularly-sampled time series. In *NeurIPS*, pages 5321–5331, 2019. 2

[35] Andrei A. Rusu, Dushyant Rao, Jakub Sygnowski, Oriol Vinyals, Razvan Pascanu, Simon Osindero, and Raia Hadsell. Meta-learning with latent embedding optimization. In *ICLR*, 2019. 2

[36] Jiawei Shen, Zhuoyan Li, Lei Yu, Gui-Song Xia, and Wen Yang. Implicit euler ODE networks for single-image dehazing. In *CVPRW 2020*, pages 877–886. IEEE, 2020. 2

[37] Jake Snell, Kevin Swersky, and Richard S. Zemel. Prototypical networks for few-shot learning. In *NeurIPS*, pages 4077–4087, 2017. 2

[38] Yonglong Tian, Yue Wang, Dilip Krishnan, Joshua B. Tenenbaum, and Phillip Isola. Rethinking few-shot image classification: A good embedding is all you need? In *ECCV*, volume 12359, pages 266–282, 2020. 2

[39] Ashish Vaswani, Noam Shazeer, Niki Parmar, Jakob Uszkoreit, Llion Jones, Aidan N. Gomez, Łukasz Kaiser, and Illia Polosukhin. Attention is all you need. In *NeurIPS*, pages 5998–6008, 2017. 5

[40] Yikai Wang, Chengming Xu, Chen Liu, Li Zhang, and Yanwei Fu. Instance credibility inference for few-shot learning. In *CVPR*, pages 12833–12842, 2020. 2, 7

[41] Wanqi Xue and Wei Wang. One-shot image classification by learning to restore prototypes. In *AAAI*, pages 6558–6565, 2020. 1, 2, 7, 8

[42] Ling Yang, Liangliang Li, Zilun Zhang, Xinyu Zhou, Erjin Zhou, and Yu Liu. DPGN: distribution propagation graph network for few-shot learning. In *CVPR*, pages 13387–13396, 2020. 1, 2, 7

[43] Shuo Yang, Lu Liu, and Min Xu. Free lunch for few-shot learning: Distribution calibration. In *ICLR*, 2021. 2

[44] Baoquan Zhang, Xutao Li, Yunming Ye, Zhichao Huang, and Lisai Zhang. Prototype completion with primitive knowledge for few-shot learning. *CoRR*, abs/2009.04960, 2020. 1, 2

[45] Chi Zhang, Yujun Cai, Guosheng Lin, and Chunhua Shen. Deepemd: Few-shot image classification with differentiable earth mover’s distance and structured classifiers. In *CVPR*, pages 12200–12210. IEEE, 2020. 2

[46] Jian Zhang, Chenglong Zhao, Bingbing Ni, Minghao Xu, and Xiaokang Yang. Variational few-shot learning. In *ICCV*, pages 1685–1694. IEEE, 2019. 2

[47] Yujia Zheng, Siyi Liu, Zekun Li, and Shu Wu. Cold-start sequential recommendation via meta learner. In *AAAI*, pages –, 2021. 1

[48] Imtiaz Masud Ziko, Jose Dolz, Eric Granger, and Ismail Ben Ayed. Laplacian regularized few-shot learning. In *ICML*, volume 119, pages 11660–11670, 2020. 2, 7